

UNCLASSIFIED

AD 423991

DEFENSE DOCUMENTATION CENTER

FOR

SCIENTIFIC AND TECHNICAL INFORMATION

CAMERON STATION ALEXANDRIA, VIRGINIA



UNCLASSIFIED

NOTICE: When government or other drawings, specifications or other data are used for any purpose other than in connection with a definitely related government procurement operation, the U. S. Government thereby incurs no responsibility, nor any obligation whatsoever; and the fact that the Government may have formulated, furnished, or in any way supplied the said drawings, specifications, or other data is not to be regarded by implication or otherwise as in any manner licensing the holder or any other person or corporation, or conveying any rights or permission to manufacture, use or sell any patented invention that may in any way be related thereto.

423991



TYCO LABORATORIES, INC.

BEAR HILL, WALTHAM 54, MASSACHUSETTS

AREA CODE 617

TELEPHONE: 899-1650

5 853100

19

AD No. _____
DDC FILE COPY

6
ELECTROCHEMISTRY OF FUEL CELL ELECTRODES.

Surface Oxidation of Gold Electrodes

by

10
S. B. Brummer and A. C. Makrides ,

fac

Technical Memorandum No. 6

Contract No. Nonr-3765(00)

dated April 16, 1962

as amended

expiring April 15, 1965

ARPA Order No. 302-62

Project Code 9800

DDC
RECEIVED
DEC 4 1963
TISIA B

October, 1963

prepared for:

OFFICE OF NAVAL RESEARCH

Materials Sciences Division

Washington 25, D. C.

423991

NO OTS

ABSTRACT

↓

The surface oxides formed on electropolished gold by potentiostatic anodization in the range 1.2 - 1.8 v vs. H^+/H_2 in the same solution, ~~have been~~ ^{WERE} studied by galvanostatic reduction at current densities between 10 and 1000 ~~$\mu a/cm^2$~~ ^{$\mu a/cm^2$} . Molar perchlorate solutions of pH 0.04 to 2.1 were employed. The extent of oxide formation is determined by the potential of anodization, the charge increasing linearly with the potential of formation in the range of 1.4 to 1.8 v. Cathodic chronopotentiograms show that reduction of the oxide occurs at a definite potential which depends on the cathodic current density. Current-potential curves, constructed from the chronopotentiograms, follow a Tafel relation with a slope of 41 mV. The exchange current for oxide reduction decreases with pH and with increasing potential of formation of the oxide. The electrochemical order of the reduction reaction is -1.65 with respect to pH. A mechanism for reduction is suggested in which it is assumed that the reduction of an intermediate (Au^{II}) is the slow step in the overall process.

~~* microamperes~~
* microamperes/sq cm

INTRODUCTION

The formation and reduction of surface oxides on metal electrodes have not been studied extensively, although both processes are of major importance in determining the kinetics of basic electrochemical reactions, for example, of the reactions involving the O_2/H_2O couple. Of particular interest are noble metals, often used as oxygen electrodes, where the absence of dissolution reactions facilitates greatly the interpretation of current-potential relations for surface oxidation. The present study deals mainly with the kinetics of reduction of surface oxides formed on gold, a metal which is unusual in its stability towards oxidation at low temperatures.

The oxidation of gold has not received as much attention as that of platinum and is not, at present, well characterized. A number of studies have been made using chronopotentiometry⁽¹⁻⁷⁾. Of particular interest is the work of Laitinen and Chao⁽¹⁾ who combined potentiostatic techniques with galvanostatic measurements and established the steady state concentration of oxide as a function of potential. The final surface species is believed to be Au_2O_3 (perhaps hydrated) (e. g. ⁽⁷⁾), but there is disagreement concerning the presence⁽⁵⁾ or absence^(1, 4) of lower valent oxides. Although the surface coverage with oxidized species during galvanostatic oxidation has frequently been examined⁽²⁻⁸⁾, apparently no attempt has been made to examine the kinetics of the reduction of the oxides of gold. In the present work, the kinetics of reductions of films formed potentiostatically have been studied over a range of pH.

EXPERIMENTAL

The principal experimental technique involved the potentiostatic oxidation of the electrode surface followed by reduction with constant current. Potential-time measurements were also made during anodic charging and during free decay from various surface oxidation conditions.

A three-compartment electrolytic cell, constructed of Pyrex glass, contained the working electrode in the central compartment and had sufficient volume to minimize concentration changes during an experiment. A Haber-Luggin capillary led to the reference electrode which was a

platinized platinum cylinder immersed in a solution saturated with purified hydrogen. The counter electrode was a roughened gold cylinder and was connected to the main compartment via a coarse fritted disc. All electrodes were mounted in such a way that only glass and Teflon came in contact with solution⁽⁹⁾.

Gold electrodes, of "spectroscopically standardized" material (Johnson, Matthey and Co.), were in the form of cylinders of area $\sim 0.8 \text{ cm}^2$. Immediately before use, the electrodes were electropolished in a cyanide bath⁽¹⁰⁾ using a current density of $\sim 6 \text{ A/cm}^2$. The specimens were polished until they showed no evidence of surface marking when viewed under a low power microscope. They were then washed in chromic-sulfuric acid, triply distilled water, and finally with the test solution. The electrodes usually retained their luster at the completion of a series of oxidation experiments and only rarely did polishing affect the measured roughness factor of the electrodes after the first couple of treatments. Geometric areas were estimated immediately after the experiments, using a micrometer. All results are given in terms of the geometric area of the electrodes.

Solutions were made up with triply distilled water (once from alkaline permanganate) and were molar with respect to ClO_4^- . Different acidities were obtained using appropriate quantities of HClO_4 (Baker Analyzed Reagent) and NaOH (Baker Analyzed Reagent). The pH was varied from 0.04 (N HClO_4) to 2.1. The working and counter electrode chambers were flushed with a continuous slow stream of N_2 , which had first passed through traps packed with glass beads cooled in liquid O_2 . Connections were made with Teflon tubing and all stockcocks, required to control the rate of gas flow, had Teflon barrels. The experimental results were not affected by stirring during the anodization or during the subsequent reduction of the film.

Potential control was maintained with a Wenking fast-rise potentiostat. Switching to a galvanostatic circuit was performed with a mercury-wetted relay (Western Electric 275C). Constant current was supplied by batteries in series with large resistances and was measured with a Greiback microammeter (type 510) to a precision of 1/2%. The potential during forced decay was measured on a Tektronix type 561A oscilloscope with a type 2A63 vertical amplifier a type 2B67 time base.

Potentials could be read to 1 mv using a sensitive scale on the

oscilloscope and a Leeds and Northrup potentiometer to back off most of the potential developed between the working and reference electrodes. Potential measurements during free decay were made with a Leeds and Northrup direct reading pH meter (input impedance $> 10^{12} \Omega$).

Reproducibility of charge with a given electrode was usually $\pm 2\%$, but between different experiments scatter up to $\pm 5\%$ was observed, probably because of differences in the surface roughness of the electrodes. The reproducibility of the potential during reduction was usually within the precision of measurement (± 1 mv) during a given experiment, and often was as good between different experiments. More usually, a variation of ± 2 mv was observed between different electrodes. All potentials are referred to the reversible H^+/H_2 potential in the same solution unless otherwise noted.

All observations were made at room temperature, $23 \pm 2^\circ C$.

RESULTS AND DISCUSSION

Anodic Charging Curves

In Fig. 1, a typical charging curve is presented. It is seen that the potential rises steeply at first and then at about 1.28 v, the exact value depending on the applied current density, a sharp break occurs. This is followed by a short region (20-30 mv) during which the potential rises quite slowly with time and then a much longer range (1.3 to 1.75 v) where the potential increases more rapidly with time. The potential becomes steady at about 1.8 v and this, no doubt, corresponds to steady-state oxygen evolution. The anodic charge during the period from the first break to 1.8 v is somewhat less than the charge which is measured cathodically after potentiostatic pre-treatment (for 5 min., see below) at 1.8 v. However, the general shape of the charge vs. potential curves found from anodic curves is the same as that obtained by cathodic reduction after potentiostatic oxidation. The anodic charging curves are similar to those reported by Hickling⁽⁴⁾, but differ in some respects from those reported by Laitinen and Chao⁽¹⁾. Hickling asserts that the total charge preceding oxygen evolution is equivalent to a monolayer of Au_2O_3 (perhaps hydrated). We do not find this. Our results and those of Laitinen and Chao⁽¹⁾ show that the amount of oxide on the surface increases smoothly with potential without any breaks corres-

ponding to various stoichiometries. Also, there are no arrests corresponding to the formation of Au^{I} or Au^{II} oxides.

Reduction Curves

Galvanostatic reduction curves of films formed potentiostatically at potentials ranging from 1.2 - 1.8 v were determined at various cathodic current densities. Measurements were not extended above 1.8 v to avoid permanent damage to the electrode (1) resulting in part, perhaps, from extensive oxidation at the grain boundaries (11). A series of runs in which the time of anodization was varied showed that the charge obtained after 5 min. and after 20 min. of anodic oxidation differed by less than 0.5%. Since the reproducibility of the charge determinations was no better than this, all oxidations were carried out for 5 min., which was sufficient to establish a steady state.

In Fig. 2 are presented two typical cathodic chronopotentiograms. These were determined after the electrode had been oxidized potentiostatically at 1.55 v for 5 min. It is seen that in contrast to anodic curves, a clear and, initially, well-defined arrest is observed corresponding to the onset of the reduction of the film. After a time, (indicated by the arrow in the top diagram in Fig. 2), corresponding to reduction to less than about 0.8 of a monolayer of adsorbed O^{2-} ($\sim 450 \mu\text{coul}/\text{cm}^2$), the potential falls rapidly. Eventually, the rate of change of potential corresponds to double layer charging, and this is followed by an arrest, not shown, where H_2 is evolved.

The method of calculating the transition time, τ , is indicated on the first curve of Fig. 2 and the method of estimating the potential of reduction is shown in the second, magnified, trace. If the reduction were commenced from less than about 1.35 v, the arrest corresponding to the reduction of adsorbed oxygen was less distinct and the calculation of the charge, q , less exact. Also, it was no longer possible to determine with any precision the initial potential of reduction. If the reduction was started from 1.65 v or above, a slight (2-5 mv) overshoot (less positive values) of the potential was observed. In this case, the potential of reduction was estimated both at the overshoot and at the arrest. The latter, while probably more valid, was more difficult to estimate accurately, so that there

was more scatter in the current-potential curves for reduction. Therefore, the results reported relate to the overshoot.

At pH of 1 and above, the charge is independent of the cathodic current density, which is expected if impurity effects are negligible (no effect of stirring) and if the dissolution rate of the film is also negligibly small. However, in more acid solutions the charge decreased linearly with increase in τ . (Fig. 3). The equivalent rate of loss of charge is about $3 \mu\text{A}/\text{cm}^2$ at pH 0.04. This zero order decay is suggestive of a dissolution reaction, whereby the oxide disappears non-electrochemically (no charge transfer) into solution. That this could not have been the case was shown by direct measurement of the rate of dissolution of the oxide. The electrode was left at open circuit for various times after anodization and the oxide remaining at the end of this time was reduced galvanostatically. A dissolution rate of about $0.3 \mu\text{A}/\text{cm}^2$ determined in this way is in good agreement with the results of Laitinen and Chao⁽¹⁾ and of Vetter and Berndt⁽⁶⁾. Thus, the q vs. τ relation at $\text{pH} < 1$ is not caused by simple chemical dissolution, but must be due to the decomposition of some active intermediate produced during electrochemical reduction. This is discussed in more detail below. In solutions where q varied with τ the reported steady state charges were estimated by extrapolating the q vs. τ line ($i \sim 30$ to $400 \mu\text{A}/\text{cm}^2$) to $\tau = 0$.

Variation of Charge with Potential and pH

The cathodic charge in N HClO_4 is shown as a function of potential of anodization in Fig. 4. It is seen that above 1.4 v the charge increases almost linearly with potential. The charge at 1.4 v is close to that for a monolayer, $450 \mu\text{C}/\text{cm}^2$ according to Hickling⁽⁴⁾. In fact, if we regard the charge at the transition point in the q vs. E curve as corresponding to a monolayer, we would suggest that a monolayer of adsorbed oxygen would be equivalent to ~ 400 rather than $450 \mu\text{C}/\text{cm}^2$. The agreement with the results of Laitinen and Chao⁽¹⁾ is excellent above ~ 1.35 v but, whereas they find a long, slow fall in the amount of surface charge at lower potentials, we observe a rapid decrease in this region, the charge becoming too small to measure at 1.2 v. Although the measurement is very difficult to

make and is inaccurate once the charge is less than about $300 \mu\text{C}/\text{cm}^2$, the shape of the cathodic curves is substantiated at other pH's and is also similar to that of the anodic charging curves. Therefore, we conclude that no significant amount of oxide or of adsorbed oxygen is present on Au below 1.2 v.

The charge-pH relationships are shown in Fig. 5 for various potentials. It is seen that the main factor which determines q is the formation potential vs. the reversible hydrogen (or possibly against the $\text{H}_2\text{O}/\text{O}_2$ potential) in the same solution rather than the potential against a pH insensitive couple. There is a slight increase in the charge at any given potential vs. the H^+/H_2 couple in the same solution as the pH is raised from 0 to 0.5, but there is essentially no change above this.

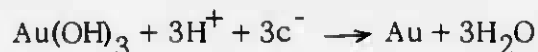
Kinetics of Oxide Reduction

A typical series of reduction curves for gold oxide formed at different anodic potentials is shown in Fig. 6. Usually, the current potential curves were determined in the current density range $30 - 200 \mu\text{A}/\text{cm}^2$ and, in general, the deviations from the Tafel plots were ± 1 mv. Experiments in the more acid solutions showed that these plots were linear at least over the range $10 - 1000 \mu\text{A}/\text{cm}^2$. As the pH was raised, however, the Tafel plots tended to curve in the direction of greater polarization. The current densities at which curvature was observed were substantially below those corresponding to the diffusion limited current for hydrogen ion. At pH 2.1, the current-potential lines were so curved as to vitiate any simple analysis of their slopes. The following discussion is mainly concerned with the linear Tafel plots obtained from pH 0.04 to pH 1.7.

The slope of the Tafel lines, 41 mv, was virtually independent of the potential of formation, although there was a slight tendency towards higher slopes (42 - 45 mv) when the oxide was formed at 1.75 and 1.8 v. The slope was also independent of pH in the range 0.04 to 1.70. In order to estimate an exchange current, i_0 , for reduction, we must know the reversible potential for the reaction and this presupposes that we have some knowledge of the composition of the oxide. The charge vs. potential curves are smooth, once a monolayer of oxide has been put down, and give no indication of the composition of the oxide. Hickling⁽⁴⁾ claims that his charging curves show that Au_2O_3 (perhaps hydrated) is the surface material. However,

the results of this work and of Laitinen and Chao⁽¹⁾ show clearly that while this conclusion may be correct, it does not follow from Hickling's experiments. If this were the case, one would expect a sharp change in the q vs. E plots at $\sim 600 - 675 \mu\text{C}/\text{cm}^2$, and this is not observed.

The reversible potential for the reaction



is given by Latimer⁽¹²⁾ as 1.45 v (reduction potential), but experimentally^(5, 13, 14) it has been found to be about 1.36 v. Laitinen and Chao⁽¹⁾ observed rest potentials, after oxide formation, of about 1.30 v and state that this results from a potential determining reaction whose reversible potential is sufficiently close to 1.36 v to assume that the oxide is very similar to Au(OH)_3 . In fact, they find it reasonable to consider the surface oxide as $\text{AuOOH}(\text{Au}_2\text{O}_3 \cdot \text{H}_2\text{O})$, see Jirsa and Buryanek⁽¹⁵⁾. The most stable normal oxide of gold is Au_2O_3 (in its various hydrated forms) and even this is thermodynamically unstable and decomposes relatively readily⁽⁷⁾. Lower oxides are known, viz. AuO ^(16, 17), but it has been shown⁽⁷⁾ that experiments^(3, 5, 18) suggesting the anodic formation of lower oxides are incorrect and are probably the result of base metal impurities, probably Fe. Thus, there is no a priori reason for assuming any well-defined stoichiometry. Certainly, it is not found for platinum (Feldberg, Enke and Bricker⁽¹⁹⁾) and indeed it has been suggested⁽¹⁹⁾ that the similarity in the anodic behavior of various noble metals may best be understood by considering the process as essentially the oxidation of water with the products being stabilized by adsorption on the metal. However, platinum and gold adsorb oxygen (or form surface oxides) at potentials which differ by nearly 0.5 v, so that it is doubtful whether such a "simplification" is particularly useful.

Decay curves (Fig. 7) show (a) that the "rest" potential is a function of the potential of formation, (b) that this potential varies with pH (Fig. 8), and (c) that frequently there is an overshoot in the decay curve (Fig. 9). Since there is little doubt that the ultimate anodic product is Au^{III} oxide⁽⁷⁾, one expects that the higher the potential of formation, the closer to 1.36 v would be the rest potential. In fact, the opposite is true. We may recall that the higher the potential of formation of the oxide, the harder it is to

reduce, Fig. 9. These observations, taken together, suggest that the rest potential is a mixed potential.

Although there is no clear justification for assuming any stoichiometry for the oxide, it is apparent that the potential of the oxide-gold couple is close to the potential of the $\text{Au}(\text{OH})_3/\text{Au}$ couple. For the purpose of compiling i_0 's, it will be assumed that the reversible potential is that of the $\text{Au}/\text{Au}(\text{OH})_3$ couple, 1.36 v, although the surface oxide may not be as completely hydrated as this.

The ease of reduction of the oxide depends on the potential at which it is formed, although it is not clear at first whether this is an effect of the potential of formation, or a result of differences in thickness. We observe that a shift of +50 mv in the potential of formation causes a shift in the reduction curve towards more negative values of about 7 mv. Therefore, a second question which arises in connection with the i_0 values is whether the exchange current for reduction is determined by the potential of formation of the oxide or by the thickness of the film. The following experiment was performed to answer this question. The metal was oxidized at a certain potential and then left on open circuit. Observations were made of the charge left on the oxide and, also, of the potential of reduction of the oxide at a given current density as a function of time on open circuit. If the determining factor for the kinetics of reduction is the thickness, we expect the potential of reduction to become more positive (in the reported experiment, by about 40 mv) as the charge on the electrode decays away. If, however, the potential of formation controls the kinetics of reduction (and hence the exchange current), we would not expect much change as the charge decayed away. Observations were made in a region where the surface coverage changed from about 1.4 monolayers to about 0.7 monolayers. The reduction potential became very slightly (5 mv) more negative, which clearly shows that the potential of formation and not the thickness of the oxide is controlling the reduction kinetics. Fig. 10 shows a plot of $\log i_0$ vs. the potential of formation. A series of straight lines is found, the lines being displaced by changes in pH.

The pH dependence of the current at a fixed potential vs. the standard hydrogen electrode is shown in Fig. 11. $\log i$ varies linearly with pH according to $(\partial \log i / \partial \text{pH})_E = -1.65 \pm 0.10$. No significant variation in $(\partial \log i / \partial \text{pH})_E$ is found with changes of either q or of the potential of formation.

GENERAL DISCUSSION

To describe the mechanism of the reduction of gold oxide, we should, in all, have to account for the following facts:

(a) A Tafel slope of 41 mv is observed independent of thickness or potential of formation.

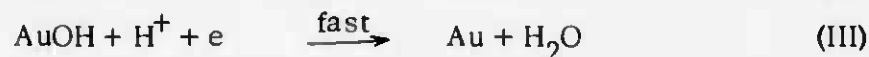
(b) $(\partial \log i / \partial \text{pH})_E$ is - 1.65 independent of thickness or potential of formation.

(c) The oxide becomes harder to reduce the higher the potential of formation, i. e., the exchange current (calculated at 1.36 v) decreases with increasing potential of formation.

(d) In more acid solutions, the charge decreases linearly with increase in the transition time, at a rate in excess of that observed for simple dissolution of the oxide.

For the present we will assume, after Laitinen and Chao⁽¹⁾, that the oxide is essentially AuOOH ($\text{Au}_2\text{O}_3 \cdot \text{H}_2\text{O}$). A simple way of accounting for a Tafel slope of about 40 mv is to assume a three-electron reduction. However, aside from the inherent improbability of such a step, the pH dependence of the reduction rate rules out this mechanism.

A likely mechanism which satisfies (a) - (c) above is given by the following sequence of reactions:



where AuO is written as the Au^{II} oxidation state and AuOH as the Au^{I} oxidation state, but neither of these postulates is necessary. The rate equation is:

$$i = 3 k_{11} (\text{AuO}) (\text{H}^+) \exp\left(-\frac{\alpha \phi F}{RT}\right) \quad (\text{I})$$

where α , the transfer coefficient, is ~ 0.5 , and ϕ is the potential. We can solve for (AuO) by assuming that reaction (I) is fast and is in equilibrium at all potentials. Then,

$$\vec{k}_I (\text{AuOOH}) (\text{H}^+) \exp\left(-\frac{\alpha \phi F}{RT}\right) = \overset{\leftarrow}{k}_I (\text{AuO}) (\text{H}_2\text{O}) \exp\left(\frac{(1-\alpha)\phi F}{RT}\right) \quad (2)$$

and

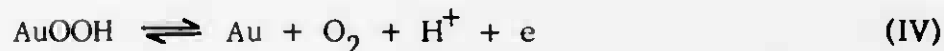
$$(\text{AuO}) = K (\text{AuOOH}) (\text{H}^+) \exp\left(-\frac{\phi F}{RT}\right) \quad (3)$$

where K is a constant equal to $\frac{\vec{k}_I}{\overset{\leftarrow}{k}_I (\text{H}_2\text{O})}$. Then the final rate equation is:

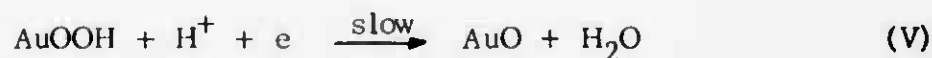
$$i = 3k_{II} K (\text{AuOOH}) (\text{H}^+)^2 \exp\left(-\frac{(1+\alpha)\phi F}{RT}\right) \quad (4)$$

Thus, if α is 0.5, the Tafel slope is 39 mv, in good agreement with experiment, $(\partial \log i / \partial \text{pH})_\phi$ as given by Eq. (4) is -2. This result is in moderate agreement with the experimental observation of $(\partial \log i / \partial \text{pH})_E = -1.65$. The most serious disadvantage of this mechanism is the assumption that the reduction of Au^{II} is the slow step. Sidgwick⁽²⁰⁾ expresses the opinion that Au^{II} compounds are really complex molecules containing equal proportions of Au^{I} and Au^{III} . Although the evidence for this view is not strong, one has some doubts about postulating this form of gold as being so relatively stable. However, the large and unusual force field in a thin adsorbed layer could alter the relative stabilities of the various oxidation states.

An alternative to this scheme which yields the same Tafel slope and pH dependence can be constructed if it is assumed that the concentration of AuOOH is fixed by the equilibrium



and that the rate limiting step is



Reaction (V) is followed by reactions (II) and (III), which are now assumed to be fast. This mechanism assumes that reaction (IV) is fast and reversible at potentials of ~ 1.2 v in 1 N HClO_4 , i.e., it requires that the reduction of oxygen on gold proceed at a rate greater than $1000 \mu\text{A}/\text{cm}^2$

(the observed reduction rate of the oxide) at these potentials. This is contrary to what is known about the reduction of osyven on gold⁽²¹⁾. In addition, this mechanism predicts a substantial effect for oxygen while, in fact, no difference was observed either in the reduction potentials or in the amount of oxide present on the surface when oxygen was bubbled over the electrode. These arguments rule out this alternative mechanism.

Exchange currents were calculated on the assumption that the reversible potential is 1.36 v vs. the reversible hydrogen electrode. On this basis (from Fig. 10) we derive the relationship:

$$i_o = 8.5 \times 10^{-3} (H^+)^{0.33} \exp\left(-\frac{0.20 F E_a}{RT}\right) (\text{amps/cm}^2) \quad (5)$$

where E_a is the potential of formation of the oxide in volts vs. the reversible hydrogen electrode in the same solution. The numerical constant (8.5×10^{-3}) relates to the choice of the reversible potential and would vary if the reversible potential were different. The only additional assumption in constructing Eq. (5) is that the reversible potential of the oxide varies by 0.059 v vs. S. H. E. per unit of pH. Eq. (4) can be used to derive the pH dependence of i_o on this same assumption. It predicts $d \log i_o / d \text{pH} = 0.50$ which is in fair agreement with the value of 0.33 found experimentally.

Comparisons of Eqs. (4) and (5) shows that the activity of (AuOOH) depends on the potential of formation according to $(\text{AuOOH}) = C \exp\left(\frac{-0.20 F E_a}{RT}\right)$. This relation essentially expresses the qualitative observation made above, that the ease of reduction of the oxide decreases with the potential of formation, and suggests that the structure of the oxide (e. g., concentration of defects) depends on the potential of its formation. There is, unfortunately, no direct evidence bearing on the composition or structure of very thin oxides formed anodically, so that it is not possible to deduce from the kinetics the structural changes which might take place.

The pH dependence of the rest potential of oxidized electrodes is in general agreement with the mechanism suggested above. If the rest potential is a mixed potential involving an impurity couple, and if the reduction rate of the impurity is essentially controlled by its rate of diffusion to the electrode, then we expect the rest potential to vary by about 95 mv per pH unit, which is in fair agreement with the observed pH dependence (85 mv vs.

S. H. E.). The overshoot phenomenon (Fig. 9) is similar to the overshoot observed in forced decay and probably arises from the same cause, i. e., from an additional potential drop (possibly ohmic) within the oxide.

The observed variation of q with the reduction current in the more acid solutions is not easily accounted for. As shown above, the dependence of q on τ cannot be explained in terms of dissolution of the oxide, but must be attributed to the decomposition of an intermediate formed during forced reduction. According to the proposed mechanism, Au^{III} and Au^{II} are in equilibrium at all potentials and, therefore, also at the potential established during free decay. Consequently, any decomposition reaction involving these species must be present during both forced and free decay, and cannot, therefore, give rise to the much higher rate of dissipation of charge during forced decay. This argument implies that Au^{I} is the unstable species. The reaction in question is obviously not the disproportionation to Au and Au^{III} , which is a well known reaction⁽²²⁾, since such a process does not dissipate charge but merely alters the kinetics of reduction. The most likely path for charge dissipation is, then, reaction of Au^{I} with H_2O to yield O_2 , which diffuses away.

SUMMARY AND CONCLUSIONS

1. The kinetics of reduction of anodic oxide films formed on gold electrodes at potentials between 1.4 and 1.8 v follow a Tafel relation with a slope of 41 mv. The exchange current (determined by extrapolation to a potential of 1.36 v vs. H^+/H_2 in the same solution) is in the range of 10^{-7} to 10^{-9} amp/cm²; it decreases with increasing anodic potentials of formation of the film and with increasing pH.

2. The electrochemical reaction order for reduction is - 1.65 with respect to pH.

3. A mechanism for reduction is suggested in which it is assumed that Au^{II} and Au^{III} are in equilibrium at all potentials and that the electrochemical reduction of Au^{II} is the slow step. This reaction scheme accounts for the main experimental results.

References

1. H.A. Laitinen and M. S. Chao, *J. Electrochem. Soc.*, 108, 726 (1961)
2. G. Armstrong, F.R. Himsworth and J.A.V. Butler, *Proc. Roy. Soc. (London)*, A134, 89 (1934)
3. G. Deborin and B. Ershler, *Acta Physicochim.*, 13, 347 (1940)
4. A. Hickling, *Trans. Faraday Soc.*, 42, 518 (1946)
5. S.E.S. El Wakkad and A.M. Shams El Din, *J. Chem. Soc.*, 3098 (1954)
6. K.J. Vetter and D. Berndt, *Z. Elektrochem.* 62, 378 (1958)
7. D. Clark, T. Dickinson and W.N. Mair, *Trans. Faraday Soc.*, 55, 1937 (1959)
8. F.G. Will and C.A. Knorr, *Z. Elektrochem.*, 64, 270 (1960)
9. M. Stern and A.C. Makrides, *J. Electrochem. Soc.*, 107, 782 (1960)
10. W.J. McG. Tegart, "The Electrolytic and Chemical Polishing of Metals", Pergamon Press, 1959, p. 62 (first method given)
11. H.A. Laitinen and C.G. Enke, *J. Electrochem. Soc.*, 107, 773 (1960)
12. W.H. Latimer, "Oxidation Potentials", Prentice-Hall, 2nd Ed., 1952
13. R.H. Gerke and M.D. Rourke, *J. Am. Chem. Soc.*, 49, 1855 (1927)
14. T.F. Buehrer and W.E. Roseveare, *ibid*, 49, 1989 (1927)
15. F. Jirsa and O. Buryanek, *Z. Elektrochem.* 29, 126 (1923)
16. F. Schottlander, *Ann.*, 217, 337 (1883)
17. G. Krüss, *ibid*, 237, 296 (1887)
18. J.K. Lee, R.N. Adams, and C.E. Bricker, *Anal. Chim. Acta*, 17, 321 (1957)
19. S.W. Feldberg, C.G. Enke and C.E. Bricker, *J. Electrochem. Soc.*, 110, 826 (1963)
20. N.V. Sidgwick, "The Chemical Elements and Their Compounds", Oxford University Press, 1962
21. G. Bianchi, G. Caprioglio, S. Malaguzzi, F. Mazza, and T. Mussini, Air Force Office of Scientific Research, Technical Report 60-299, May, 1960
22. T.F. Buehrer, F.S. Wartman and R.L. Nugent, *J. Am. Chem. Soc.*, 49, 1272 (1927)

FIGURE CAPTIONS

- FIG. 1 Typical anodic chronopotentiogram in 1 N HClO₄.
- FIG. 2 Typical cathodic chronopotentiogram in 1 N HClO₄ after 5 minutes of anodization at controlled potential. Arrow in upper Figure indicates ~ 0.8 monolayer of O²⁻ remaining on surface. Arrow in lower Figure indicates the potential corresponding to the reduction of the oxide.
- FIG. 3 The variation of the cathodic charge with time of reduction in 1 N HClO₄.
- FIG. 4 Variation of cathodic charge with the potential of anodization in 1 N HClO₄. Open and closed circles are from different experiments in the present study. Crosses are from the results of Laitinen and Chao⁽¹⁾. The arrow indicates a monolayer.
- FIG. 5 Charge vs. pH at various potentials of formation.
- FIG. 6 Current-potential curves for reduction of films formed at various potentials.
- FIG. 7 Decay curves of oxides formed at various potentials.
- FIG. 8 Decay curves of oxides formed at 1.6 v as a function of pH.
- FIG. 9 Open circuit potential as a function of the amount of oxide on the surface.
- FIG. 10 Exchange currents for oxide reduction as a function of the potential of formation and pH.
- FIG. 11 The rate of reduction of oxides formed at various potentials as a function of pH.

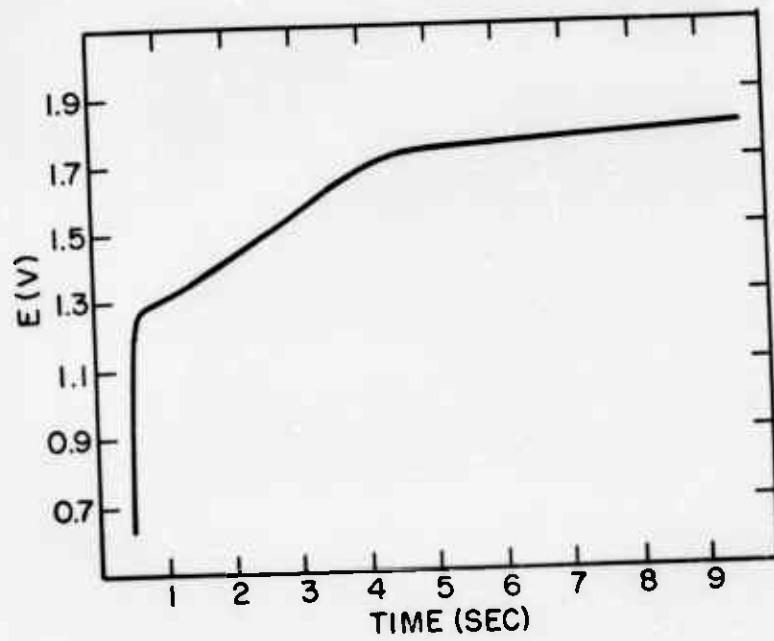


FIG. 1

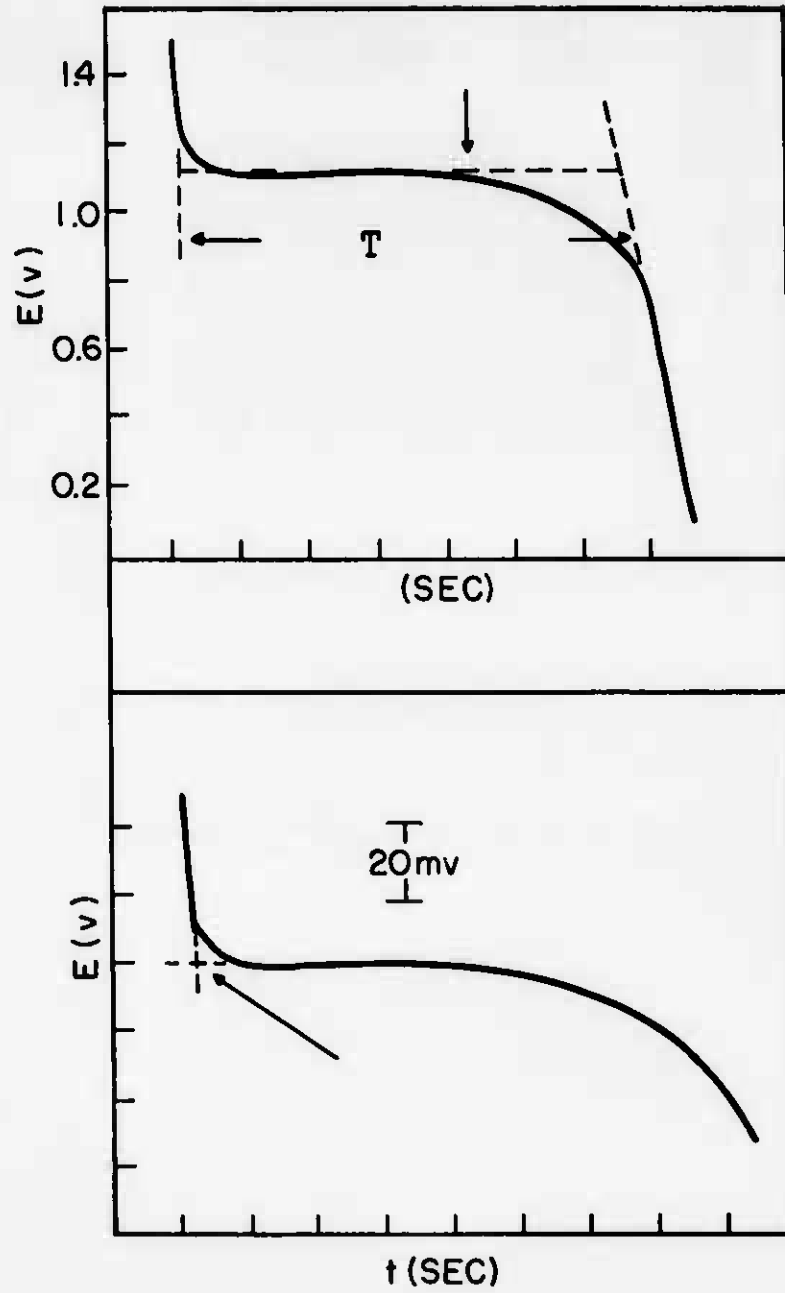


FIG. 2

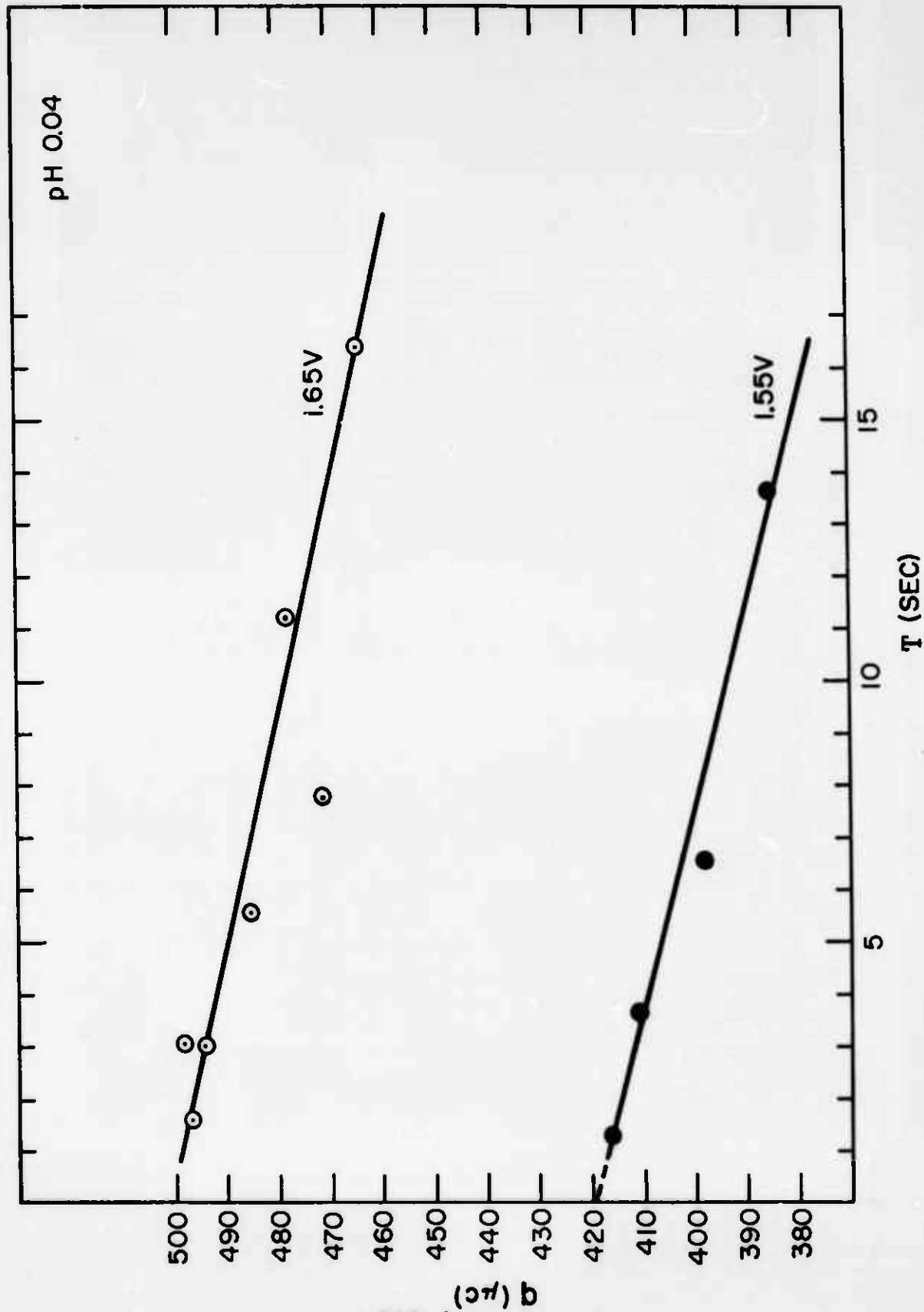


FIG. 3

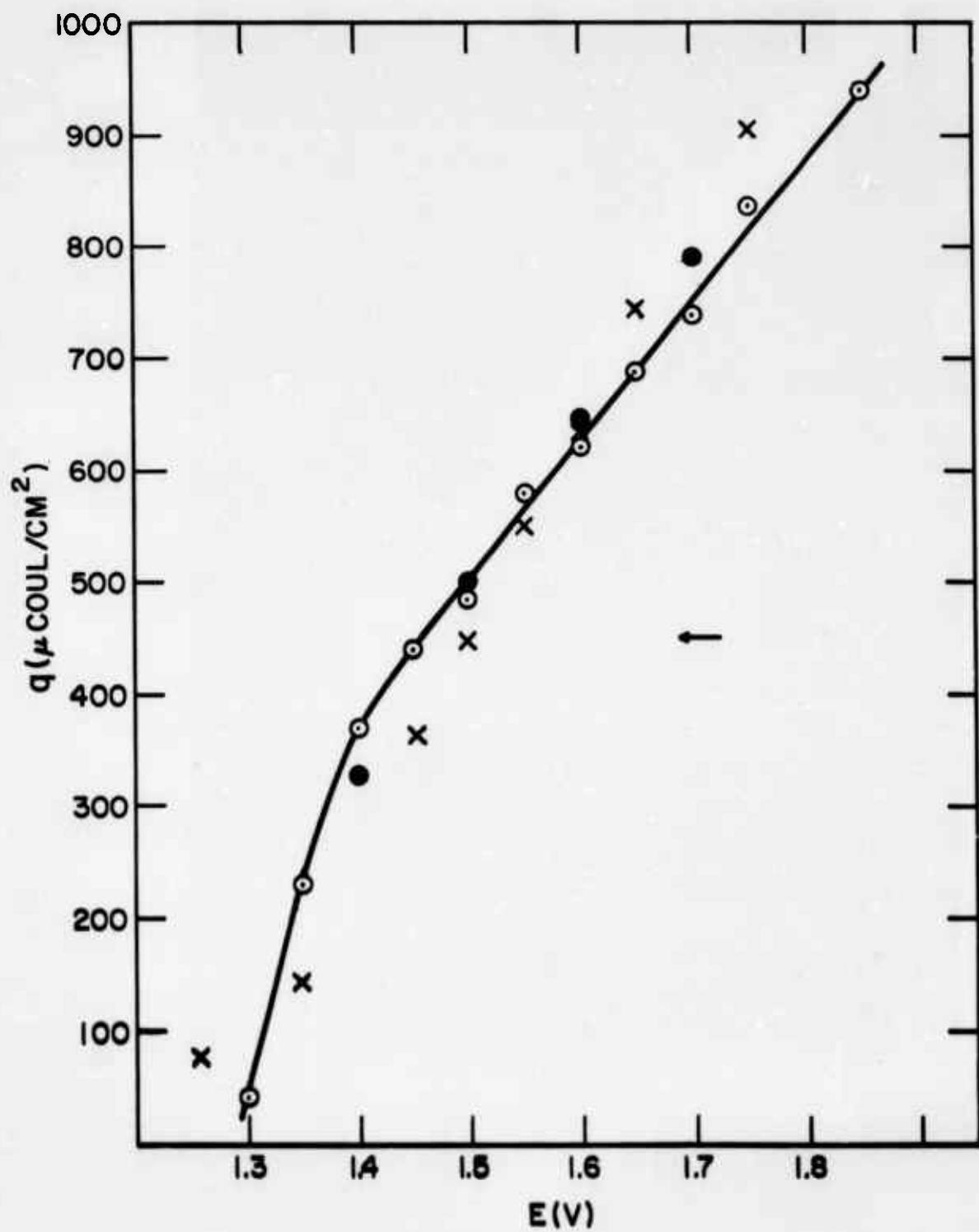


FIG. 4

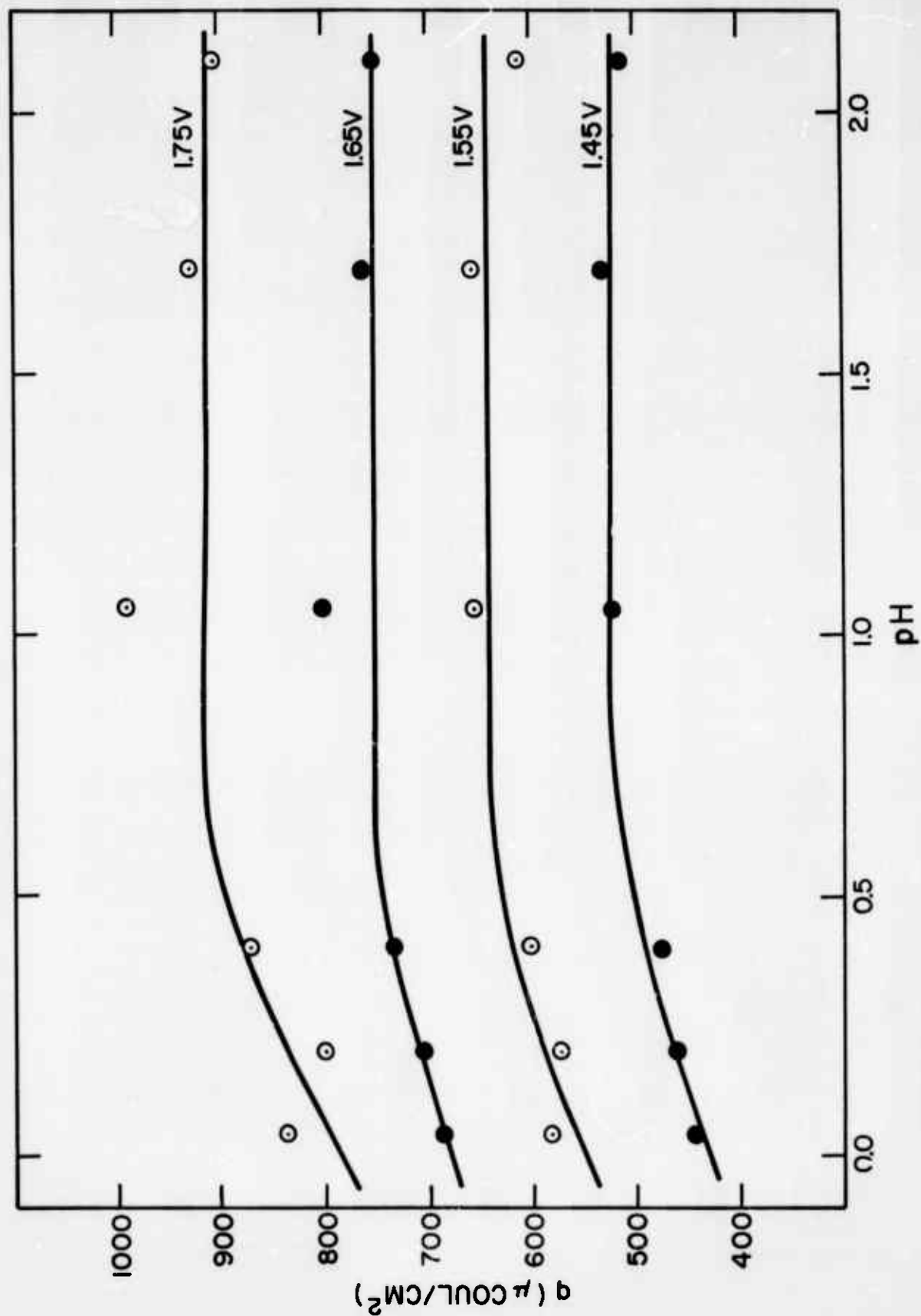


FIG. 5

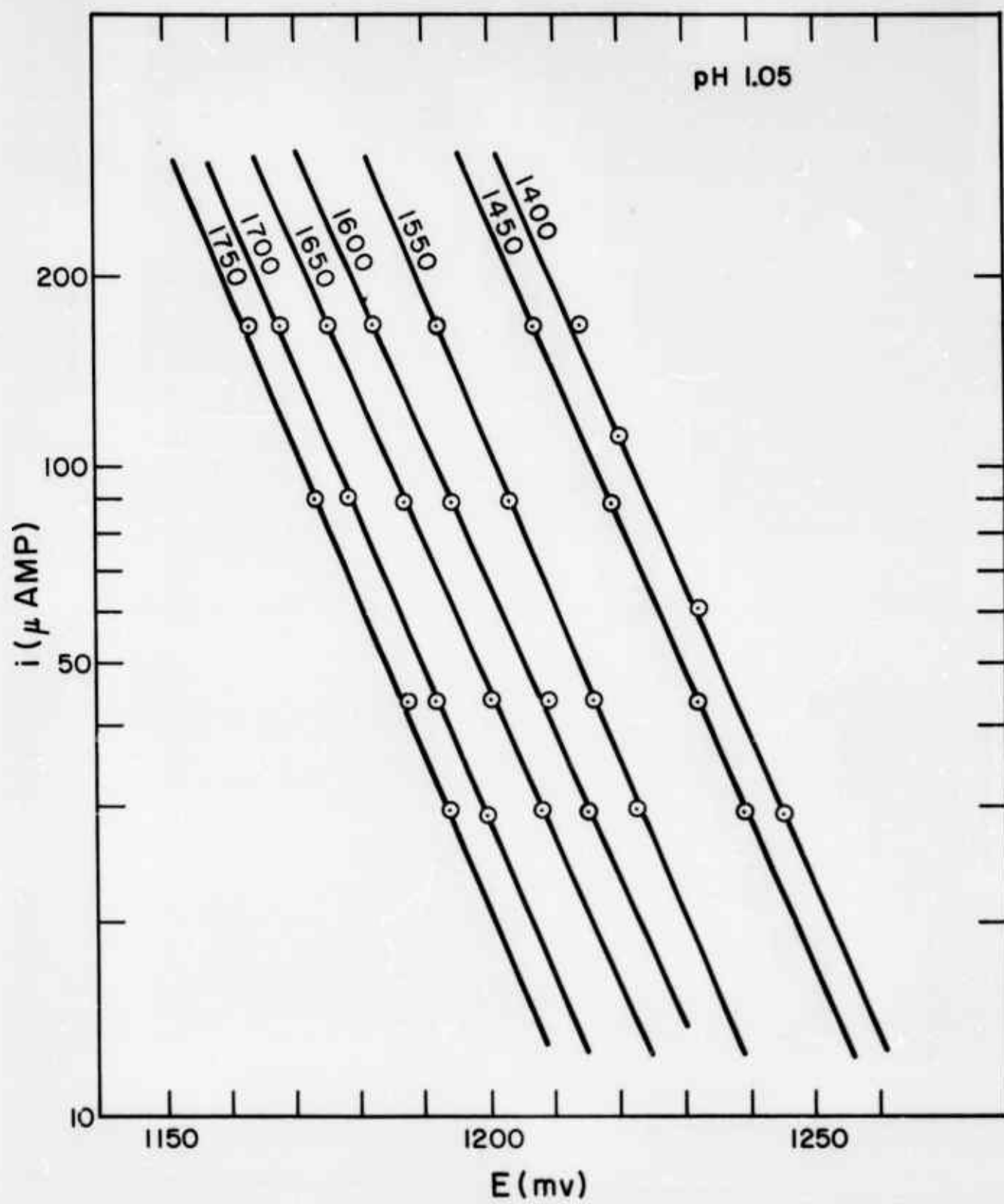


FIG. 6

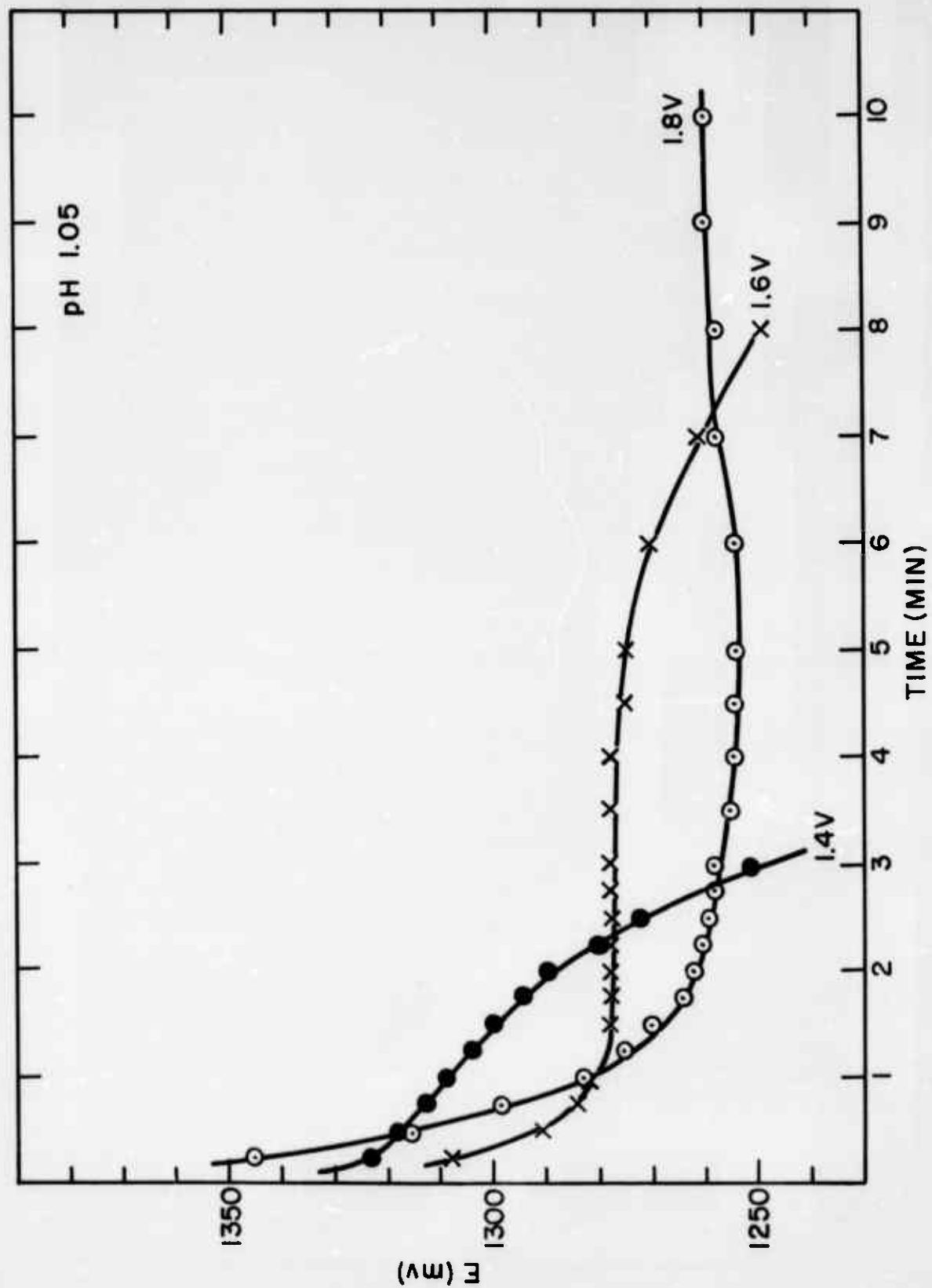


FIG. 7

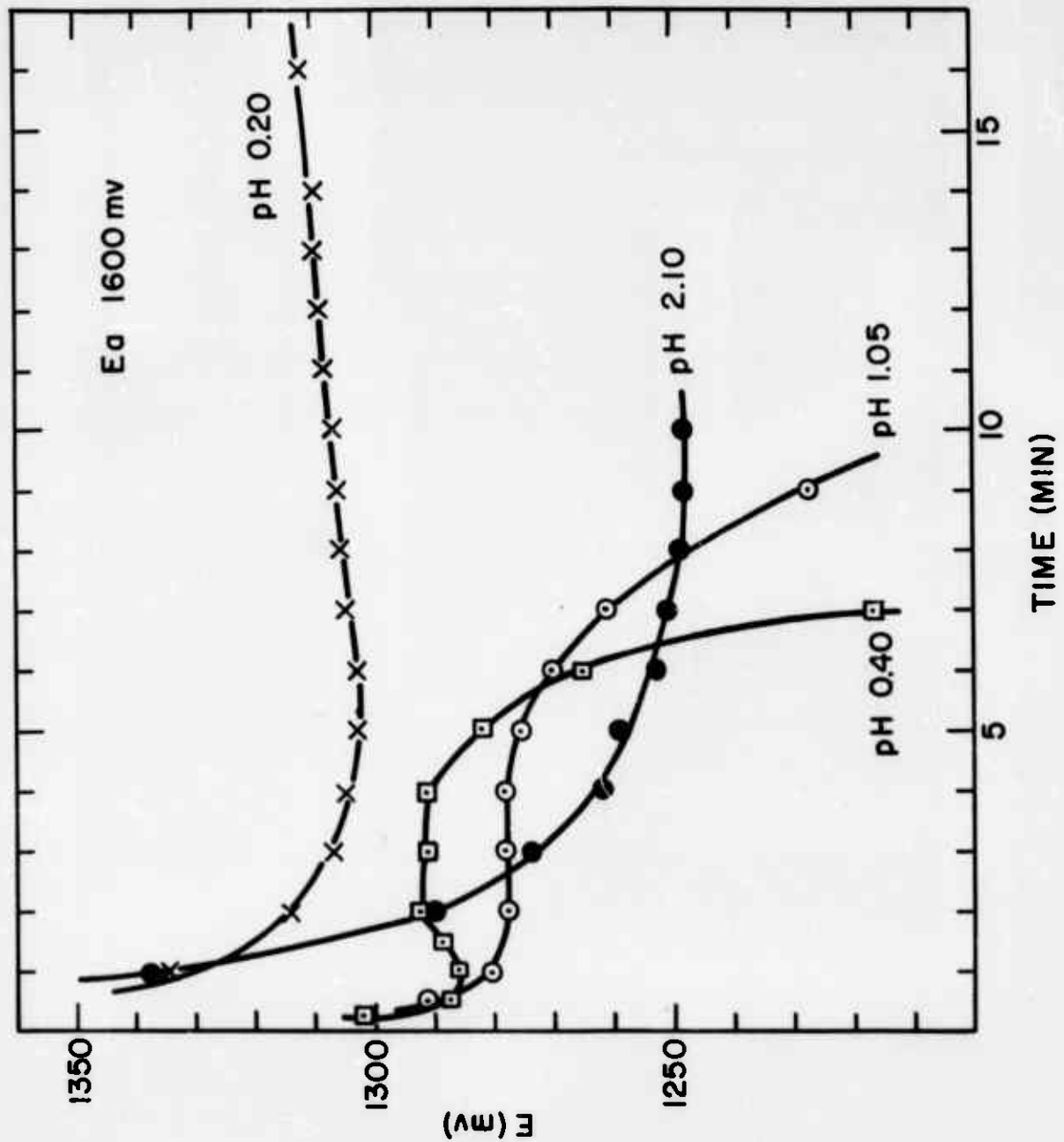


FIG. 8

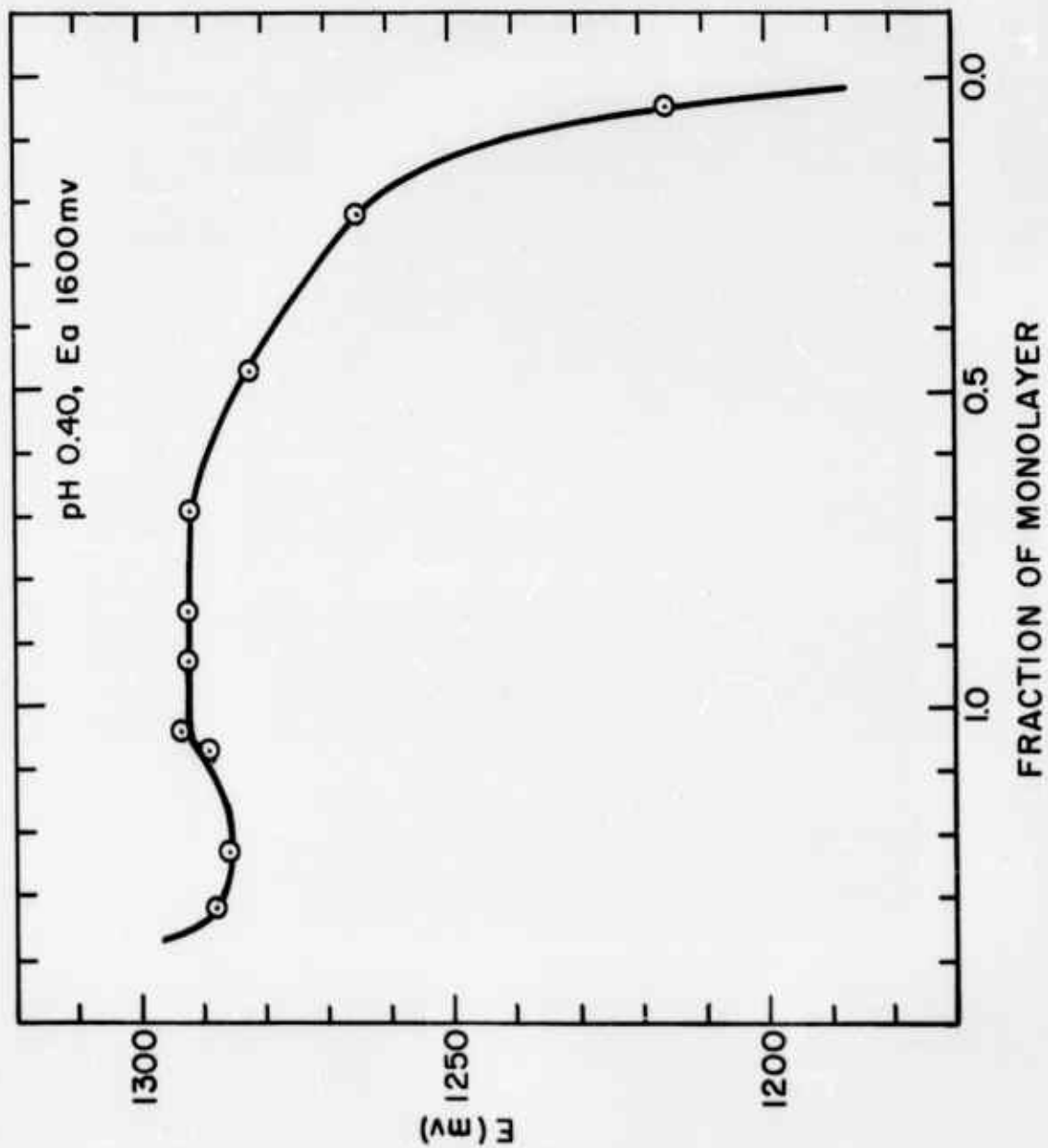


FIG. 9

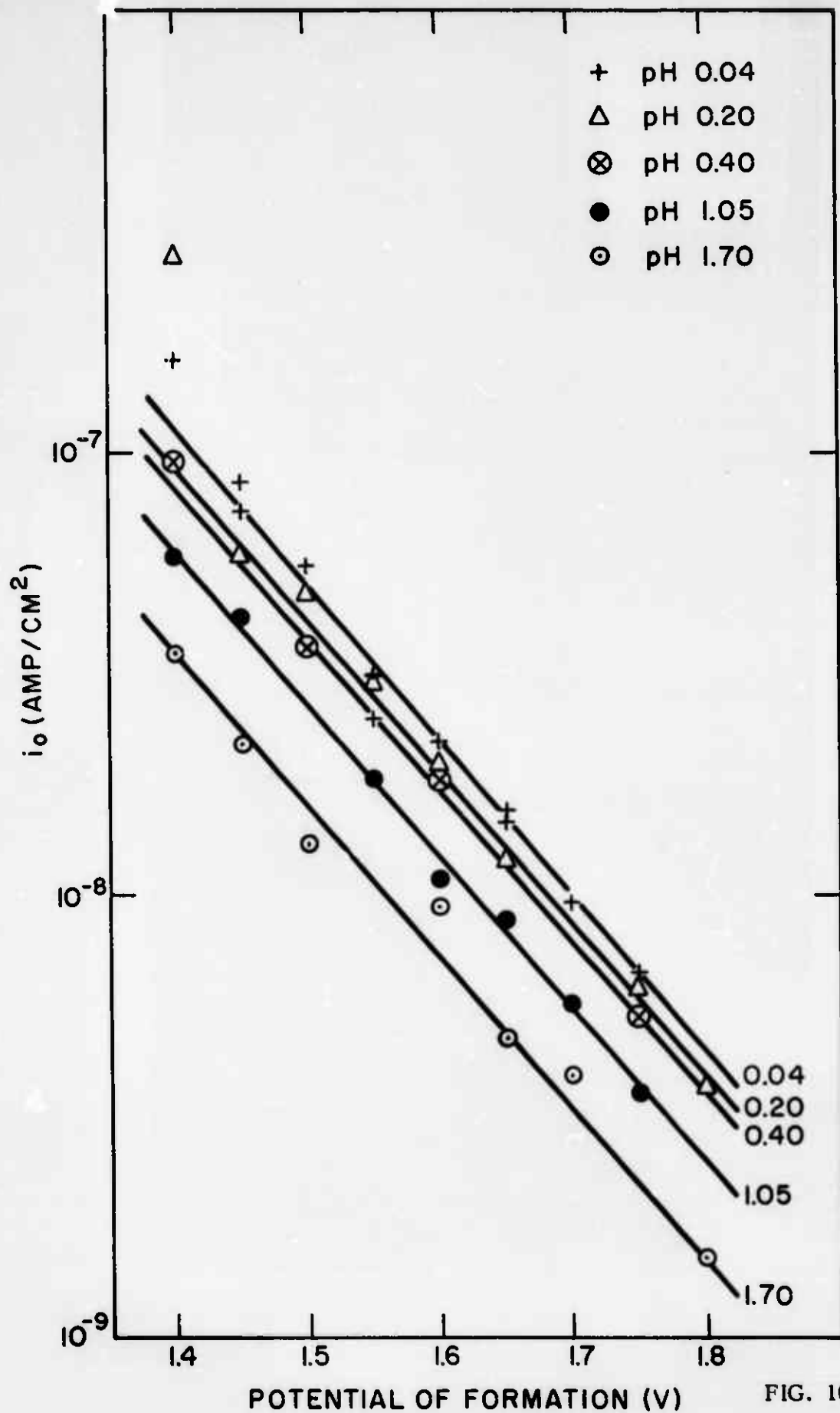


FIG. 10

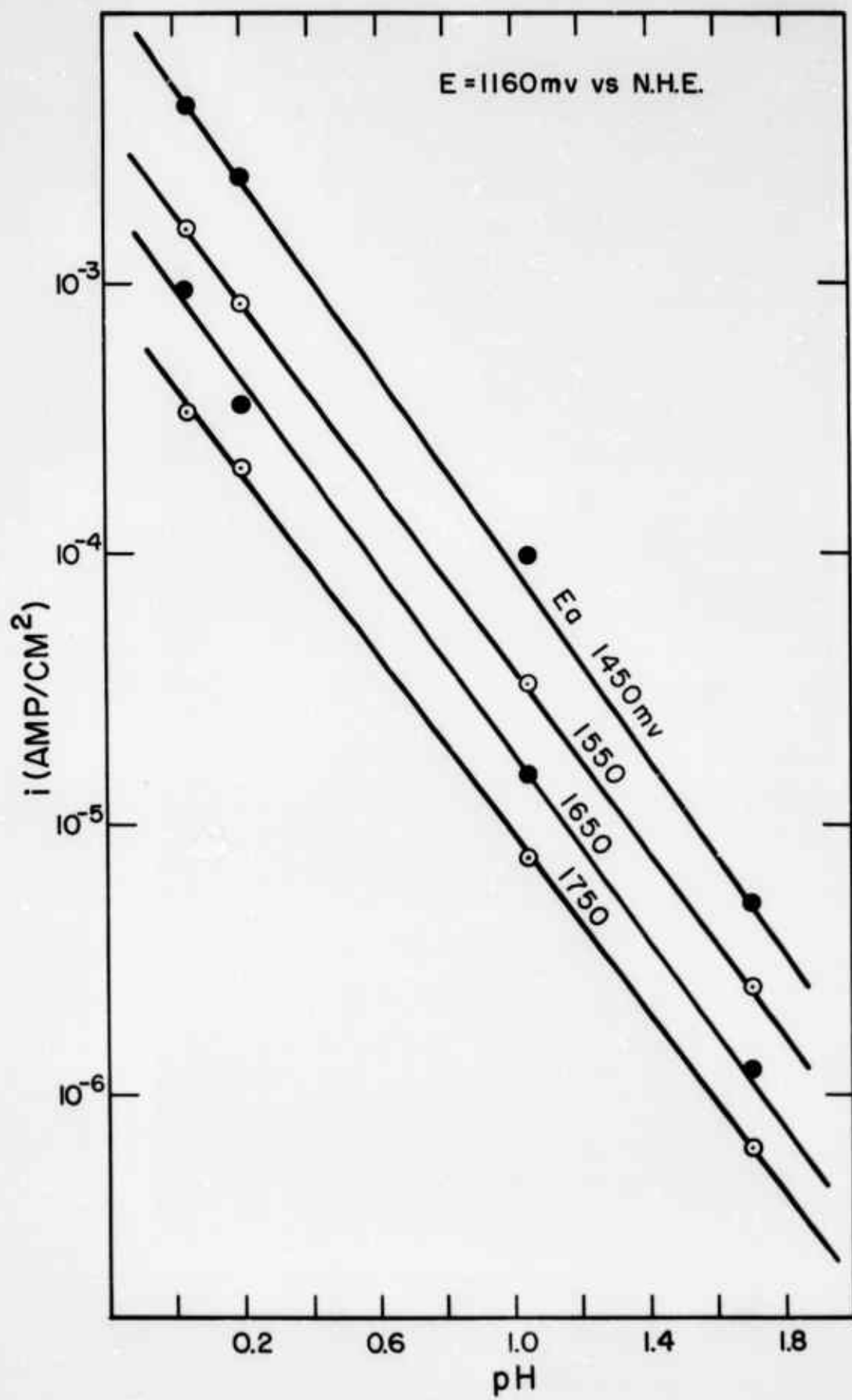


FIG. 11

TECHNICAL REPORT DISTRIBUTION LIST

Contract No. Nonr 3765 (OO)

Commanding Officer Office of Naval Research Branch Office 230 N. Michigan Avenue Chicago 1, Illinois (1)	Harry Diamond Laboratories Washington 25, D. C. Attn: Library (1)
Commanding Officer Office of Naval Research Branch Office 207 West 24th Street New York 11, New York (1)	Office, Chief of Research & Development Department of the Army Washington 25, D. C. Attn: Physical Sciences Division(1)
Commanding Officer Office of Naval Research Branch Office 1030 East Green Street Pasadena 1, California (1)	Chief, Bureau of Ships Department of the Navy Washington 25, D. C. Attn: Code 342A (2)
Commanding Officer Office of Naval Research Branch Office Box 39, Navy #100, F. P. O. New York, New York (7)	Technical Library, DL1-3 Bureau of Naval Weapons Department of the Navy Washington 25, D. C. (4)
Director, Naval Research Laboratory Washington 25, D. C. Attn: Technical Information Officer (6) Chemistry Division (2)	Defense Documentation Center Cameron Station Alexandria, Virginia (20)
Chief of Naval Research Department of the Navy Washington 25, D. C. Attn: Code 425 (2)	Commanding Officer U. S. Army Electronics Research and Development Laboratory Attn: SELRA/DR Fort Monmouth, New Jersey 07703 (1)
DDR&E Technical Library Room 3C-128, The Pentagon Washington 25, D. C. (1)	Naval Radiological Defense Laboratory San Francisco 24, California Attn: Technical Library (1)
Department of the Army Supply & Maintenance Command Maintenance Readiness Division Washington 25, D. C. Attn: Technical Director (1)	Naval Ordnance Test Station China Lake, California Attn: Head, Chemistry Div. (1)
U. S. Army Natick Laboratories Clothing & Organic Materials Division Natick, Massachusetts Attn: Associate Director (1)	Commanding Officer Army Research Office Box CM, Duke Station Durham, North Carolina Attn: CRD-AA-IP (1)

Atomic Energy Commission Division of Research Chemistry Programs Washington 25, D. C.	(1)	Dr. Howard L. Recht Astropower, Inc. 2968 Randolph Avenue Costa Mesa, California	(1)
Atomic Energy Commission Division of Technical Information Extension Post Office Box 62 Oak Ridge, Tennessee	(1)	Mr. L. R. Griffith California Research Corporation 576 Standard Avenue Richmond, California	(1)
Commanding Officer U. S. Army Chemical Research and Development Laboratories Attn: Librarian Edgewood Arsenal, Maryland	(1)	Dr. Ralph G. Centile Monsanto Research Corporation Boston Laboratories Everett 49, Massachusetts	(1)
Commanding Officer ONR Branch Office 495 Summer Street Boston 10, Massachusetts	(1)	Mr. Ray M. Hurd Texas Research Associates 1701 Guadalupe Street Austin 1, Texas	(1)
Director, ARPA Attn: Dr. J. H. Huth Material Sciences Room 3D155 The Pentagon Washington 25, D. C.	(4)	Dr. C. E. Heath Esso Research & Engineering Company Box 51 Linden, New Jersey	(1)
Dr. S. Schuldiner Naval Research Laboratory Code 6160 Washington 25, D. C.	(1)	Dr. Richard H. Leet American Oil Company Whiting Laboratories Post Office Box 431 Whiting, Indiana	(1)
Dr. A. B. Scott Department of Chemistry Oregon State University Corvallis, Oregon	(1)	Dr. Douglas W. McKee General Electric Company Research Laboratories Schenectady, New York	(1)
Inspector of Naval Material 495 Summer Street Boston 10, Massachusetts	(1)	Dr. E. A. Oster General Electric Company, DECO Lynn, Massachusetts	(1)
Mr. R. A. Osteryoung Atomics International Canuga Park, California	(1)	Dr. R. R. Heikes Solid State Phenomena Dept. Westinghouse Electric Corporation Pittsburgh, Pennsylvania	(1)
Dr. David M. Mason Stanford University Stanford, California	(1)	Professor Herman P. Meissner Massachusetts Institute of Technology Cambridge 39, Massachusetts	(1)

Mr. Donald P. Snowden General Atomic Post Office Box 608 San Diego 12, California	(1)	Dr. B. R. Sundheim Department of Chemistry New York University New York 3, New York	(1)
Mr. C. Tobias Chemistry Department University of California Berkeley, California	(1)	Dr. E. M. Cohn NASA Code RPP 1512 H Street, N. W. Washington 25, D. C.	(1)
Mr. Y. L. Sandler Westinghouse Research Laboratories Schenectady, New York	(1)	Dr. E. Yeager Department of Chemistry Western Reserve University Cleveland 6, Ohio	(1)
Dr. Paul Delahay Department of Chemistry Louisiana State University Baton Rouge, Louisiana	(1)	Dr. V. I. Matkovich The Carborundum Company Niagara Falls, New York	(1)
Dr. W. J. Hamer Electrochemistry Section National Science Foundation Washington 25, D. C.	(1)	Dr. A. M. Zwickel Department of Chemistry Clark University Worcester, Massachusetts	(1)
Dr. Herbert Hunger Power Sources Division U. S. Army Signal Research & Development Laboratory Fort Monmouth, New Jersey	(1)	Dr. Michael O'Keefe Department of Chemistry Arizona State University Tempe, Arizona	(1)
Dr. T. P. Dirkse Department of Chemistry Calvin College Grand Rapids, Michigan	(1)	Lockheed Aircraft Corporation Missiles and Space Division Technical Information Center 3251 Hanover Street Palo Alto, California	(1)
Dr. George J. Janz Department of Chemistry Rensselaer Polytechnic Institute Troy, New York	(1)	Dr. G. C. Szego Institute for Defense Analysis 1666 Connecticut Avenue, N. W. Washington 9, D. C.	(1)
Mr. N. F. Blackburn E. R. D. L. Materials Branch Fort Belvoir, Virginia	(1)	Dr. R. F. Baddour Department of Chemistry Massachusetts Institute of Technology Cambridge 39, Massachusetts	(1)
Mr. W. M. Lee, Director Contract Research Department Pennsalt Chemicals Corporation 900 First Avenue King of Prussia, Pennsylvania	(2)		

Technical Report Distribution List

Page 4

Mr. T. W. Cushing, Manager
Military Service Department
Engelhard Industries, Inc.
113 Astor Street
Newark, New Jersey (1)

Thompson Ramo Wooldridge Inc.
23555 Euclid Avenue
Cleveland 17, Ohio
Attn: J. Ed Taylor (1)
Associate Director, RD&E

Aerospace Corporation
Post Office Box 95085
Los Angeles 45, California
Attn: Library Technical
Documents Group (1)

Dr. Galen R. Frysinger
Electric Power Branch
E. R. D. L.
Fort Belvoir, Virginia (1)